https://doi.org/10.5194/gmd-2021-109
Preprint. Discussion started: 4 May 2021

Geoscientific Model Development Discussions

Incorporation of volcanic SO_2 emissions in the Hemispheric CMAQ (H-CMAQ) version 5.2 modeling system and assessing their impacts on sulfate aerosol over Northern Hemisphere

Syuichi Itahashi[1], Rohit Mathur[2], Christian Hogrefe[2], Sergey L. Napelenok[2], and Yang Zhang[3]

[1] Environmental Science Research Laboratory, Central Research Institute of Electric Power Industry (CRIEPI), 1646 Abiko, Abiko, Chiba 270–1194, Japan
[2] Center for Environmental Measurement and Modeling, Office of Research and Development, U.S. Environmental Protection Agency, Research Triangle Park, NC 27711, U.S.A.
[3] Department of Civil and Environmental Engineering, Northeastern University, Boston, MA 02115, U.S.A.

Correspondence to: Syuichi Itahashi (isyuichi@criepi.denken.or.jp)

Abstract

The state-of-the-science Community Multiscale Air Quality (CMAQ) Modeling System has recently been extended for hemispheric-scale modeling applications (referred to as H-CMAQ). In this study, satellite-constrained estimation of the degassing SO_2 emissions from 50 volcanos over the northern hemisphere is incorporated into H-CMAQ, and their impact on tropospheric sulfate aerosol (SO_4^{2-}) levels is assessed for 2010. The volcanic degassing improves predictions of observations from the Acid Deposition Monitoring Network in East Asia (EANET), the United States Clean Air Status and Trends Network (CASTNET), and the United States Integrated Monitoring of Protected Visual Environments (IMPROVE). Over Asia, the increased SO_4^{2-} concentrations were seen to correspond to the locations of volcanoes, especially over Japan and Indonesia. Over the U.S.A., the largest impacts occurred over the central Pacific caused by including the Hawaiian Kilauea volcano while the impacts on the continental U.S.A. were limited to the western portion during summertime. The emissions of the Soufriere Hills volcano located on Montserrat Island in the Caribbean Ocean affected the southeastern U.S.A. during the winter season. The analysis at specific sites in Hawaii and Florida also confirmed improvements in regional performance for modeled SO_4^{2-} by including volcanoes SO_2 emissions. At the edge of the western U.S.A., monthly-averaged SO_4^{2-} enhancements greater than 0.1 μg/m^3 were noted within the boundary layer (defined as surface to 750 hPa) during June-September. Investigating the change on SO_4^{2-} concentration throughout the free troposphere revealed that although the considered volcanic SO_2 emissions occurred at or below the middle of free troposphere (500 hPa), compared to the simulation without the volcanic source, SO_4^{2-} enhancements of more than 10% were detected up to the top of the free troposphere (250 hPa). Our model simulations and comparisons with measurements across the Northern Hemisphere indicate that the degassing volcanic SO_2 emissions are an important source impacting airborne sulfur budgets and should be considered in air quality model simulations assessing background SO_4^{2-} levels and their source attribution.

https://doi.org/10.5194/gmd-2021-109
Preprint. Discussion started: 4 May 2021

Geoscientific Model Development Discussions

1 Introduction

Airborne sulfate (SO_4^{2-}) is one of the major components of tropospheric particulate matter worldwide (Zhang et al., 2007) and plays important roles in modulating the earth-atmosphere energy budget, atmospheric circulation, cloud properties, and precipitation (Seinfeld and Pandis, 2016). SO_4^{2-} is produced via the aqueous- and gas-phase oxidation of sulfur dioxide (SO_2), and these processes are well understood (Seinfeld and Pandis, 2016). The dominant sources of SO_2 emissions are attributed to anthropogenic activity (Warneck and Williams, 2012). The global anthropogenic SO_2 emissions peaked in the early 1970s with around 130 Tg/yr and then decreased; however, this emission trend has contrasting characteristics over the U.S.A. and Asia (e.g., Smith et al., 2011; Xing et al., 2015a). Anthropogenic SO_2 emissions from the U.S.A. showed a peak in the early 1970s with 30 Tg/yr and subsequently decreased (Smith et al., 2011). Publicly available observational records have begun from the late 1980s over the U.S.A., and it has been confirmed that SO_4^{2-} concentration in the U.S.A. decreased during the early 1990s through 2010 in response to these reductions in SO_2 emissions as evidenced in analyses of observational aerosol composition (e.g., Hand et al., 2012; Gan et al., 2015). On the other hand, anthropogenic SO_2 emissions across Asia, especially China, have shown a continuous increase since 1970 (Smith et al., 2011) up to 2006 and then decreased (Li et al., 2017) in response to control measures. These multi-decadal changes in SO_2 emissions have resulted in not only contrasting changes in tropospheric SO_4^{2-} levels but also in aerosol radiative effects (e.g., Wild et al., 2009; Xing et al., 2015b), their feedback on atmospheric dynamics and air quality (e.g., Xing et al., 2016), and acid deposition (e.g., Zhang et al., 2018; Mathur et al., 2020).

As SO_2 emission control is reducing regional airborne SO_4^{2-}, quantifying the relative contribution of long-range transported SO_4^{2-} and the portion attributable to natural sources is becoming increasingly important. For instance, regional haze assessments require quantification of visibility impairment that are associated with anthropogenic enhancements over natural visibility levels, which in turn necessitates accurate quantification of the contribution of natural sources. Next to the anthropogenic emissions, volcanic emissions have an important contribution to SO_2 emissions (Warneck and Williams, 2012). A time-averaged inventory of volcanic emissions was estimated as 13 Tg-SO_2/yr during early 1970s to 1997, and these volcanoes are mostly located in the Pacific Rim region (Andres and Kasgnoc, 1998). Volcanic emission fluxes can be measured in several ways such as a correlation spectrometer (COSPEC), but observable volcanic eruptions are limited in time and location. Satellite observations are now proving to be a useful approach to monitor the volcanic emissions and have provided a global volcanic SO_2 emission inventory since 1978 (Carn et al., 2016). Accurate representation of volcanic emissions requires quantification of emissions emitted from both persistent degassing and sporadic eruptions. Recently, a decadal-scale global volcanic SO_2 emissions inventory for the 2005-2015 period, constrained by the Ozone Monitoring Instrument (OMI) has been established (Carn et al., 2017). The enhanced methodology with greater sensitivity allows the detection of emissions as low as approximately 6 Gg-SO_2/yr for low-altitude volcanoes, and covers a total of 91 persistently degassing volcanic SO_2 sources. The volcanic SO_2 emissions from degassing are relatively stable at 23.0±2.3 Tg-SO_2/yr during 2005-2015, and the highest amount was approximately 26 Tg-SO_2/yr in 2010. In terms of the volcanic activity, sporadic eruptions inject into the

https://doi.org/10.5194/gmd-2021-109
Preprint. Discussion started: 4 May 2021


Geoscientific Model Development Discussions

atmosphere comparatively large amounts of SO_2 emissions. For example, one of the largest eruptions in the 1990s was that of Mt. Pinatubo in June 1991 which was estimated to have injected 18 Tg of SO_2 emissions into the atmosphere (Smithsonian Institution, 2020). The injection heights of that eruption reached to more than 30 km and caused the largest perturbations ever observed in the chemical state of the stratosphere and the earth-atmosphere radiation budget (McCormick, et al., 1995). However, such eruptive emissions are temporary. According to the comparison between the degassing and eruptive emissions, Carn et al. (2017) estimated that during 2005-2015, volcanic activity contributed about 23 Tg/yr of SO_2 due from degassing while eruptive SO_2 emissions ranged from 0.2 to 10 Tg/yr of SO_2. Therefore, understanding the behavior of the degassing SO_2 emissions and its contributions to airborne SO_4^{2-} levels is important. For example, it was reported that although volcanic SO_2 emissions contributed 15% to the total sulfur emissions, it attributed 27% of the tropospheric sulfur budget (Lamotte et al., 2020).

Numerical modeling is a useful tool to characterize source-receptor relationships. Regional modeling studies have already indicated that volcanic SO_2 emissions are one of the main sources of SO_4^{2-} over Japan (Itahashi et al., 2017a; 2017b; Itahashi, 2018; Itahashi et al., 2019). SO_2 emissions from volcanos in the Pacific Rim region not only regulate tropospheric SO_4^{2-} levels in surrounding countries but through long-range transport can also potentially impact SO_4^{2-} distributions over the Pacific and background levels in the western U.S.A. Liu et al. (2008) for instance suggest that west to east across the North Pacific, sulfate originating from East Asia sources contributed approximately 80%–20% of sulfate at the surface, but at least 50% at 500 hPa. Taking into consideration that volcanoes are mainly over the Pacific Rim area and the seasonally prevalent cross-Pacific transport patterns, volcanic SO_2 emissions could also affect SO_4^{2-} concentrations over North America. While previous studies have attempted to quantify global tropospheric SO_4^{2-} budgets (e.g., Chin et al., 1996; Chin and Jacob, 1996), the assessments are representative of conditions in the late 1980's to early 1990's. Since anthropogenic SO_2 emissions have changed significantly over the past several decades, and since recent studies provide improved constraints of volcanic SO_2 emissions, the work summarized in this manuscript attempts to assess the contributions of volcanic SO_2 emissions on tropospheric SO_4^{2-} distributions across the Northern Hemisphere and North America. We specifically focus on assessing the impacts of the persistent degassing volcanic SO_2 emissions.

This manuscript is organized as follows. In section 2, the modeling system and simulation set up are described along with the ground-based observations used to evaluate the model performance. In section 3, the model results and comparisons with observations are presented and the impact of including volcanic SO_2 emissions is discussed. Finally, section 4 summarizes the key results and limitations of this work, and discusses future perspectives.

https://doi.org/10.5194/gmd-2021-109
Preprint. Discussion started: 4 May 2021


Geoscientific Model Development Discussions

2 Methodology

2.1 Hemispheric CMAQ modeling system and its set up

The Community Multiscale Air Quality (CMAQ) modeling system version 5.2 extended for hemispheric applications (H-CMAQ) (Sarwar et al., 2015; Xing et al., 2015a; Mathur et al., 2017; Itahashi et al. 2020a, 2020b) is used to incorporate and assess the impacts from volcanic SO_2 emissions. H-CMAQ is configured to cover the entire Northern Hemisphere, utilizing a polar stereographic horizontal discretization of 187×187 grid points with a grid spacing of 108 km and a terrain-following vertical coordinate system with 44 layers of variable thickness from the surface up to 50 hPa. The emission datasets for the base case H-CMAQ simulation are based on the Hemispheric Transport of Air Pollution version 2 (HTAP2) experiments. The details were described in previous studies (Janssens-Maenhout et al., 2015; Pouliot et al., 2015; Galmarini et al., 2017; Hogrefe et al., 2018). Over the modeling domain, a total of 105.8 Tg/yr of SO_2 emissions are emitted. The spatial distribution of SO_2 emissions is shown in Fig. 1a with high SO_2 emissions from fossil fuel combustion activities in North America, Europe including western Russia, and Asia, with relatively higher amounts across regions in China and India as described in Janssens-Maenhout et al. (2015). The CMAQ configuration employed the CB05 gas-phase chemical mechanism and the aero6 module with nonvolatile primary organic aerosol (POA) (Appel et al., 2017). CMAQ treats one gas-phase oxidation and five aqueous-phase oxidations for converting S(IV) (i.e., sulfur compounds with oxidation state 4) into S(VI) (i.e., sulfur compounds with oxidation state 6). The gas-phase oxidation involves reaction with hydroxyl (OH) radical, and five aqueous-phase reactions involve oxidation by hydrogen peroxide (H_2O_2), ozone (O_3), oxygen (O_2) via Fe and Mn catalysis, methyl hydrogen peroxide (MHP), and peroxyacetic acid (PAA). The meteorological fields to drive H-CMAQ are derived from simulations with the Weather Research and Forecasting (WRF) model version 3.6.1. The WRF model is configured to use the rapid radiative transfer model for global climate models (RRTMG) radiation scheme for both longwave and shortwave (Iacono et al., 2008), Morrison double-moment scheme (Morrison et al., 2009) and the Kain-Fritsch (KF) cumulus parameterization (Kain, 2004) for microphysics and cumulus parameterization, and Mellor-Yamada-Janjic scheme for planetary boundary layer (Janjic et al., 1994). In this study, the entire year of 2010 was simulated to analyze the volcanic emission impacts over the Northern Hemisphere. The WRF simulations used nudging for wind, temperature, and water vapor fields towards NCEP final analysis (FNL) of 1° spatial and 6 h temporal resolution (NCEP, 2020) over the entire vertical model extent. WRF simulation started from 1 January 2009 to set one year spin-up time prior to the analysis period the year of 2010 as recommended by Mathur et al. (2017). The CMAQ simulation were initialized on 1 December 2009 with three-dimensional chemical fields from prior model simulations for 2010 by Hogrefe et al. (2018).

Earlier development and applications with the H-CMAQ modeling system have not considered volcanic SO_2 emissions. In this study, degassing volcanic SO_2 emissions estimated by Carn et al. (2017) are incorporated into H-CMAQ. The estimated emissions of SO_2 from the 50 volcanos within our northern hemisphere modeling domain (Figure 1b) is 12.7 Tg/yr. Table 1 provides detailed information on these 50 volcanoes including name, location (longitude and latitude), altitude (as above sea level (a.s.l.)), and SO_2 emission rate. Kilauea located in Hawaii is estimated to have the highest amount of

https://doi.org/10.5194/gmd-2021-109
Preprint. Discussion started: 4 May 2021


Geoscientific Model Development Discussions

degassing SO_2 emissions. Taking into accounts the characteristics of the degassing process, volcanic degassing SO_2 emissions were allocated into the model vertical layer corresponding to the volcano's altitude. This approach was also taken in another global model analysis (Chen et al., 1996; Ge et al., 2016). Even though in principle volcanic degassing emissions could be assigned to the first model layer because CMAQ uses a terrain following vertical coordinate system, the 108 km grid spacing used in CMAQ does not allow the model to adequately resolve localized terrain peaks such as volcanoes and assigning their emissions to the first model layer would not account for the fact that in reality these emissions typically occur above the mixed layer. Therefore, the vertical layer to which volcanic degassing emissions were assigned was determined by first calculating the difference between the altitude of a given volcano (Table 1) and the CMAQ terrain height for the cell in which it is located, and then determining the vertical CMAQ layer corresponding to this difference. A schematic of the resultant assigned vertical layer is illustrated in Fig. 2. Most of volcanoes are located between altitudes of 500-5000 m above sea level (a.s.l) (Table 1), and these correspond to layers 11-26 in the current model configuration.

2.2 Ground-based Observations

As seen from Fig. 1 (b), the majority of the degassing volcanoes are located in the Pacific Rim region and their impacts on SO_4^{2-} levels in Japan have previously been studied (Itahashi et al., 2017a, b, 2019; Itahashi, 2018). To assess model performance in the Asian region, ground-based surface SO_4^{2-} observations were obtained from the Acid Deposition Monitoring Network in East Asia (EANET) program (EANET, 2020). During 2010, filter-pack measurements of SO_4^{2-} are available at 35 EANET sites with the following geographic distribution: 1 site in China, 3 sites in the South Korea, 12 sites in Japan, 2 sites in Mongolia, 4 sites in Russia, 5 sites in Thailand, 2 sites in Vietnam, 2 sites in Philippines, 3 sites in Malaysia, and 1 site in Indonesia. Most of sites report two-week measurements, but some sites provide weekly or daily measurements. All available observation data were used in this study. As we have discussed in previous work (Itahashi et al., 2020b), Asian air pollution can impact on air quality over the U.S.A.; however, the magnitude of volcanic emissions on tropospheric SO_4^{2-} levels over North America has not been well studied. To evaluate the impact of volcanic SO_2 emissions located in the northern hemisphere on model performance, surface observations over the U.S.A. were obtained from the Clean Air Status and Trends Network (CASTNET) which covered remote and rural sites mostly over eastern U.S.A. (CASTNET, 2020) and the Integrated Monitoring of Protected Visual Environments (IMPROVE) which covered remote sites mostly over western U.S.A. (IMPROVE, 2020). Sampling frequency is weekly and daily (1-in-3 day) for CASTNET and IMPROVE, respectively. A total of 84 CASTNET sites and 170 IMPROVE sites were available in 2010. Because of the coarse resolution of H-CMAQ simulations, measurements at urban sites were not considered in this study.

https://doi.org/10.5194/gmd-2021-109
Preprint. Discussion started: 4 May 2021


Geoscientific Model Development Discussions

To evaluate model performance with ground-based observations, the Pearson's correlation coefficient (R) with student's *t*-test is used for assessing the statistical significance level. The normalized mean bias (NMB) and the normalized mean error (NME) are also calculated as follows (e.g., Zhang et al., 2006; Itahashi et al., 2020a).

$$R = \frac{\sum_1^N (O_i - \bar{O})(M_i - \bar{M})}{\sqrt{\sum_1^N (O_i - \bar{O})^2}\sqrt{\sum_1^N (M_i - \bar{M})^2}} \quad (1)$$

$$NMB = \frac{\sum_1^N (M_i - O_i)}{\sum_1^N O_i} \quad (2)$$

$$NME = \frac{\sum_1^N |M_i - O_i|}{\sum_1^N O_i} \quad (3)$$

where, N is the total observation number, O_i and M_i represent each individual observation and model result respectively, and $\bar{O}$ and $\bar{M}$ represent the arithmetical mean of observations and model results respectively. Based on a review of model performance over North America simulated by regional-scale air quality models, Emery et al. (2017) suggested threshold values of R > 0.70, NMB < ±10%, and NME < 35% as performance goal, and threshold values of R > 0.40, ±10% < NMB < ±30%, and 35% < NME < 50% as performance criteria for daily SO_4^{2-}.

3 Simulation Results and Discussion

3.1 Model Evaluation

To provide an overview of the modeling results, we first present the annual-average SO_4^{2-} simulated by the base H-CMAQ configuration in Fig. 3 (a). High concentrations of SO_4^{2-} (greater than 5 μg/m^3; red color in Fig. 3) are noted over East Asia, some parts of India, and the Arabian Peninsula corresponding to the intense SO_2 emissions shown in Fig. 1. The concentrations of SO_4^{2-} over Europe and U.S.A. were mostly 0.5-2.5 μg/m^3 (blue color to green color in Fig. 3). The performance of this base case H-CMAQ simulation was evaluated over Asia and the U.S.A through comparison with SO_4^{2-} measurements by EANET, CASTNET, and IMPROVE. The results of statistical analysis using R, NMB, and NME are listed in Table 2. Detailed maps of model results over Asia and the U.S.A. with overlaid distribution of surface observations are shown in Fig. 4. Fig. 4 also contains a scatter plot between base H-CMAQ and surface observations are also shown; data for each month is shown using a different color. Significant scatter is noted in the correlation between the modeled and observed concentrations with an R of 0.43 over Asia (Table 2). Recent analysis of 12 regional models participating in the MICS-Asia model intercomparison study (Chen et al., 2019) however also revealed moderate correlations (0.46-0.79) with EANET observation. In terms of NMB and NME, NMB was −37.6% and NME was 67.0% in this study (Table 2). MICS-Asia showed

https://doi.org/10.5194/gmd-2021-109
Preprint. Discussion started: 4 May 2021


Geoscientific Model Development Discussions

NMB of −19.1% as model ensemble mean, but ranged from −67.0% to +69.3% for individual regional models (Chen et al., 2019). The H-CMAQ basecase performance statistics were comparable or slightly worse compared to the previous regional-scale modeling studies (e.g., Itahashi, 2018; Itahashi et al., 2018; Yamaji et al., 2020; Chatani et al., 2020). This in part results from the inability of the coarse model grid resolution to resolve localized high pollution episodes as seen in the scatter-plot in Fig. 4. Over the U.S.A., the spatial distribution patterns with low SO_4^{2-} in the western U.S.A. and comparatively higher values in the eastern U.S.A. are well captured in the base H-CMAQ simulation, though the model tended to underestimate across sites in the eastern U.S.A. The observed annual averaged values by CASTNET were ranged between 2.5 and 3.4 μg/m^3 over eastern U.S.A. The scatter-plot also verified the reasonable correspondence between model and observations. A winter minimum and summer maximum is noted both in the modeled and observed SO_4^{2-} values across the U.S.A. driven by expected variations in intensity of oxidant chemistry and conversion of S(IV) to S(VI). The statistical scores of R, NMB, and NME were within or close to the performance criteria proposed by Emery et al. (2017) over the U.S.A., and were also comparable to previous regional-scale modeling studies (e.g., Zhang et al., 2009; Zhang et al., 2013). Overall, despite the use of coarse horizontal grid resolution of 108 km in H-CMAQ, model performance statistics were generally within the model performance statistics noted for other the regional modeling applications. One possible contributor to the noted SO_4^{2-} underestimation over Asian region in the base H-CMAQ could be from the missing of volcanic SO_2 emissions, especially in the Pacific Rim. The impact of introducing the degassing volcanic SO_2 emissions is further discussed in the following sections.

3.2 Impact of incorporating volcanic SO_2 emissions

The annual averaged SO_4^{2-} simulated after incorporating degassing volcanic SO_2 emission in H-CMAQ is shown in Fig. 3 (b), and the increase in concentrations relative to the base H-CMAQ is shown in Fig. 3 (c) as absolute value and in Fig. 3 (d) as the percentage change from the original H-CMAQ simulation. Impacts of including volcanic SO_2 emissions on tropospheric SO_4^{2-} are noted across the Pacific and up to the western coastline of the U.S.A. It should be noted that even though the degassing volcanic emissions are allocated to upper model layers (see, Fig. 2 and Table 1), they get transported through much of the troposphere with non-trivial impacts detected at the surface level. Increases of at least 0.1 μg/m^3 in SO_4^{2-} concentration were simulated except over central Asia, equatorial and high latitude regions, and the Atlantic ocean, and most of the U.S.A. The maximum increase of greater than 1.0 μg/m^3 on an annual average basis was seen over the central Pacific (Fig. 3(c)). This increase is primarily attributed to SO_2 emission from Kilauea in Hawaii which is estimated to have the highest degassing emissions (see Table 1). In addition, a moderate increase of up to 1.0 μg/m^3 on an annual average basis was found over the Antilles islands in the Caribbean Sea. This was related to the volcanic activity of Soufriere Hills volcano located in Montserrat (No. 5 in strength; Table 1). Compared to the broad impacts found over Pacific Rim region, the impact of incorporating degassing volcanic SO_2 emission was limited over Europe and Africa. Increased concentration ranging between 0.1-0.3 μg/m^3 simulated over southern Europe and northern Africa region were caused by volcanoes in Italy (Nos. 8 and 29 in Table 1), Ethiopia (No. 45 in Table 1), and Yemen (No. 47 in Table 1). Because only four degassing volcanoes in this region

https://doi.org/10.5194/gmd-2021-109
Preprint. Discussion started: 4 May 2021


Geoscientific Model Development Discussions

are considered in this study (see, Fig. 1 (b)), the impact itself was lower compared to other regions. In the terms of the percentage changes relative to the original H-CMAQ (depicted in Fig. 3 (d)), increased concentration greater than 1.0 μg/m^3 seen in Fig. 3 (c) corresponded to +200% change, and that of 0.1 μg/m^3 corresponded to about a +10% change. Over North America and the polar region, the increased absolute concentration was less than 0.1 μg/m^3, whereas the percentage increase change was 10-30%. For the annual average, it was found that the degassing volcanic SO_2 emissions increased SO_4^{2-} concentrations less than 0.1 μg/m^3 over the entire U.S.A. but this still represented a 10-20% increase over the western U.S.A.

The impacts on modeling performance by including volcanic SO_2 emissions are discussed based on the statistical analysis scores. In terms of the statistical analysis listed in Table 2, NMB and NME over Asia compared to EANET observation were improved, though the R values were not impacted significantly. This result was consistent with our previous findings that suggested volcanoes are an important source of tropospheric sulfur in East Asia (Itahashi et al., 2017; Itahashi, 2018). Over the U.S.A., the base H-CMAQ had better modeling performance compared to Asia, and NMB and NME were improved when volcanic degassing emissions were included but R did not change. The improvements were noticeable in the comparison with observations at IMPROVE sites located in the western U.S.A., NMB showed close agreement between H-CMAQ and IMPROVE observation. From these evaluations, it is concluded that the incorporation of degassing volcanic SO_2 emissions helps to improve performance of simulated SO_4^{2-} in H-CMAQ by a small margin.

The impacts of degassing volcanic SO_2 emissions on seasonal SO_4^{2-} distributions and long-range transport were further analyzed by examining monthly mean contributions as illustrated in Fig. 5. Similar to the annual mean distributions shown in Fig. 3 (c), the maximum impact was seen over the central Pacific associated with emissions from the Kilauea volcano throughout the year. Regarding its monthly variation, the increased concentration at the surface level during spring to summer season (from April to September) were higher than those during winter (especially, December and January). The higher impacts during summer result both from higher rates of SO_2 to SO_4^{2-} conversion as well as enhanced convective mixing. In contrast during winter lower conversion rates and a more stably stratified atmosphere result in reduced SO_4^{2-} from volcanic emissions at the surface. The enhanced SO_4^{2-} associated with emissions from the Kilauea volcano (with highest emission rate as indicted in Table 1) stretch across the central Pacific to the western shores of the U.S., with enhancements in surface-level SO_4^{2-} on a monthly-mean basis greater than 0.1 μg/m^3 across portions of the western U.S. The contribution of volcanoes located on the Kamchatca Peninsula (Nos. 2, 6, 12, 14, 16, 19 and others in Table 1) are estimated to be comparatively lower on an annual average basis, but may be higher episodically under conducive transport condition. During the winter season, the impacts from Kilauea did not reach to the western U.S.A., however, the impacts from Soufriere Hills located in Montserrat (No. 5 in Table 1) reached the southern U.S.A. Further analysis focused on specific sites is discussed in next section.

3.3 Impacts of volcanic SO_2 emissions at specific sites

Detailed analysis at an observation site located in Hawaii was further conducted to evaluate model performance. According to the observation summary (WRAP, 2020), a large fraction of the measured SO_4^{2-} at this location is attributed to

https://doi.org/10.5194/gmd-2021-109
Preprint. Discussion started: 4 May 2021


Geoscientific Model Development Discussions

SO_2 emissions associated with volcanic activity from Kilauea. A total of three IMPROVE sites are located in the state of Hawaii. One of site is located in the Hawaii Volcanoes National Park and is in vicinity of the Kilauea volcano (site name is HAVO1). Comparison of model and observed temporal variation in SO_4^{2-} at this site are displayed in Fig. 6 (a). The observation showed higher concentration during the winter season, and the average concentration through 2010 was 2.37 $\mu g/m^3$. The base H-CMAQ simulation showed largely invariant concentrations through the year with an annual average value of 0.87 $\mu g/m^3$ and a negative correlation against observation. The statistical scores of NMB showed high negative bias because the base H-CMAQ did not capture the higher concentration observed during winter. By including the degassing volcano emissions, the model showed spikes for higher concentration days. Though the observed maximum peak of 30 $\mu g/m^3$ on 3 January was not fully captured, the simulated values of around 10 $\mu g/m^3$ by incorporating the volcano emissions were significantly enhanced relative to the base model. The result showed that the averaged concentration was 2.87 $\mu g/m^3$, and NMB showed +21.2% with moderate correlation by R of 0.36. The inclusion of degassing volcanoes led to better performance at this specific site; however, the deterioration in the value of NME should be considered. While the H-CMAQ simulations with incorporated volcanoes also showed lower SO_4^{2-} concentrations during summer season compared to winter, the simulated summertime values were higher than observed and led to a persistent positive bias during this season. A potential reason for this behavior could be the treatment of degassing volcanoes SO_2 emissions as constant flux in this study. For example, a case study targeted to quantify the air quality impacts of the Kilauea eruption in 2018 showed that the importance of temporal variation of emissions and plume rise calculation (Tang et al., 2020). Our results indicate general improvements of model performance by including degassing volcano emissions represented by a constant temporal and vertical profile, but refining the treatment of these aspects should be studied in future work. In terms of SO_2 concentration, IMPROVE sites do not measure it. Based on an intensive observational study at Kilauea during January-February 2013, SO_2 concentrations showed large variations from below 1 ppbv under conditions of no influence of the volcanic plume to over 3,000 ppbv when airmasses influenced by the volcanic plume were sampled (Kroll et al., 2015). In the base H-CMAQ calculation, the daily averaged SO_2 mixing ratios for the grid cell with the Kilauea volcano ranged from below 0.01 to 0.14 ppbv, while the annual mean value was 0.03 ppbv. In contrast, when volcanic emissions were incorporated in H-CMAQ, simulated SO_2 mixing ratios ranged from below 0.03 to 1088.20 ppbv with an annual mean value of 221.08 ppbv which better matches the dynamic range inferred from the SO_2 measurements in the vicinity of the Kilauea volcano reported in Kroll et al. (2015).

A second location-specific analysis was conducted at site located in the state of Florida. As seen in the monthly-average spatial distribution patterns (Fig. 5), the influence of volcanic activity of Soufriere Hills located in Montserrat are more prominent during winter. The southernmost measurement location in Florida (see, Fig. 4) is the CASTNET site EVE419 and comparison of modeled values with observations at this location are shown in Fig. 6 (b). The seasonal pattern with summer minima was captured by H-CMAQ but underestimated throughout the year. Increased concentrations through the incorporation of volcanic emissions are noted during January, late April to early May and December. The increase during late April to early May were not seen from the monthly-averaged spatial distribution (Fig. 5); hence these could be the episodic long-range transport by southeasterly winds. Because of these increased concentrations, all statistical scores of R, NMB, NME showed

https://doi.org/10.5194/gmd-2021-109
Preprint. Discussion started: 4 May 2021


Geoscientific Model Development Discussions

improvement compared to the base H-CMAQ. CASTNET also provides measurements of weekly-average SO_2 mixing ratios. At the EVE419 site in Florida, the observed annual mean was 0.61 ppbv whereas base H-CMAQ and H-CMAQ with volcanic SO_2 emissions both showed 0.77 ppbv. Due to the coarse horizontal grid resolution, the model tended to overestimate SO_2 levels at this remote site. Additionally, the results suggest that the SO_2 from volcanic sources was fully oxidized to SO_4^{2-} during long-range transport and there was no direct transport of SO_2 itself at this site. Collectively, these results and those summarized in Table 2 and Figure 4 suggest that inclusion of degassing volcanic emissions moderately improve model performance statistics for simulated SO_4^{2-} spatial distributions and temporal variations. Note that the incorporation of volcanic degassing emissions does not necessarily improve model performance in all instances due to the presence of uncertainties and potentially compensating errors in other parts of the modeling system (i.e. model input fields like other emissions and meteorology, model representation of processes such as chemical reactions and deposition) and suitability of the measurement network (e.g., proximity) in characterizing the variability in tropospheric composition due to volcanic degassing emissions . Nonetheless, incorporating the degassing volcanic SO_2 emissions which clearly occur in nature is an important aspect for enhancing the completeness of the modeling system itself. Quantifying the space and time variations of persistent volcanic degassing emissions on tropospheric composition is important, especially in context of using models to characterize background pollution levels and anthropogenic enhancements of tropospheric pollutants and associated health and visibility impacts.

3.4 Impact on upper troposphere

Finally, the impacts caused by including the degassing volcanoes were investigated throughout the troposphere. In subsequent analysis, the boundary layer is defined from the surface to 750 hPa, and the free troposphere is defined from 750 to 250 hPa and pressure levels of 750, 500, and 250 hPa are used to refer as the bottom, middle, and top of the free troposphere similar to our previous study (Itahashi et al., 2020b). The vertical profile of simulated SO_4^{2-} concentration averaged along the edge of western U.S.A. (defined in Fig. 4 (b)) were analyzed. The vertical profile of the base H-CMAQ and the increased concentration due to incorporating the degassing volcanic SO_2 emission are plotted in Fig. 7. Modeled SO_4^{2-} concentrations decreased from the surface to upper layers, and concentration levels were greater in summer than those during winter (e.g., Fig. 4 for surface results). Incorporation of volcanic SO_2 emissions, increased monthly mean SO_4^{2-} within the boundary layer by up to 0.4 $\mu g/m^3$ during June to September. This increase is consistent with the spatial distribution at surface depicted in Fig. 5, but also occurs through the depth of the boundary layer. During other months, the simulated concentration increases were less than 0.1 $\mu g/m^3$ throughout the free troposphere.

Simulated annual average SO_4^{2-} concentration distributions at the bottom, middle and top of the free troposphere from the two model simulations and the estimated increase due to incorporation of degassing volcanic emissions are shown in Fig. 8. The simulated spatial distribution of SO_4^{2-} exhibited similar patterns at the bottom of the free troposphere (Fig. 8 (a), (d)) with higher concentration over Asian region. However, significant differences in the magnitude and spatial distributions of simulated SO_4^{2-} between the two simulations are noted at the middle and top of the free troposphere as seen from higher

https://doi.org/10.5194/gmd-2021-109
Preprint. Discussion started: 4 May 2021


Geoscientific Model Development Discussions

concentration in the northern Pacific region close to the north pole (Fig. 8 (b), (c), (e), (f)). The maximum concentrations at the top of the free troposphere (Fig. 8 (c), (f)) decreased by a factor of 10 compared to those at the surface (Fig. 3 (a), (b)). The increased concentration by including degassing volcanoes showed the increment corresponded to the location of volcanoes. In contrast to the increased concentrations over Pacific Rim region found at the surface level (Fig. 3 (c)), increased SO_4^{2-} over the Bering Sea was noticeable at the bottom of the free troposphere (Fig. 8 (g)). Over this area, increased SO_4^{2-} ranged from +0.08 to +0.2 at the bottom of free troposphere were found. This is mainly caused by the Mutnovsky, Gorely, Kliuchevskoi, and Bezymianny volcanoes (No. 5 and No. 6 in Table 1) and other volcanoes located on the Kamchatca Peninsula (Nos. 12, 14, 16, 19, 24, 35, 36, and 48), and volcanoes over Alaska Peninsula (Nos. 37, 38, 39, 40, and 46) surrounding Bering Sea. These volcanoes were characterized by the relatively higher altitude (No. 6 was allocated into the highest altitude) considered in this study (Table 1 and Fig. 2). The increased concentration at the middle and top of free troposphere were widely distributed with centering on the north pole. These increased concentrations indicated that while volcanic emissions were assumed to be injected into the lower and middle free troposphere (Fig. 2), their impacts on secondary SO_4^{2-} production were detected throughout the free troposphere. Based on the percentage change relative to the original H-CMAQ simulation, Fig. 8 further shows that the spatial extent of the impact of including degassing volcanic SO_2 emissions on SO_4^{2-} increased with height, with most of the northern hemisphere showing increases exceeding 10% at 250 hPa.

4 Conclusions

Previous work on the development and evaluation of the H-CMAQ model has historically not considered volcanic SO_2 emissions. In this study, satellite-constrained SO_2 emissions from 50 degassing volcanoes over the northern hemisphere are incorporated into H-CMAQ, and their impacts on tropospheric SO_4^{2-} is evaluated for model simulations of the calendar year 2010. Model performance was evaluated using network observations of EANET over Asia and CASTNET and IMPROVE over U.S.A. The base H-CMAQ underestimated SO_4^{2-}, and this was partially rectified by incorporating volcanic SO_2 emissions as indicated through improvements in the statistical scores of R, NMB, and NME. Over Asia, largest increase in SO_4^{2-} were simulated in vicinity of the volcanos, especially over Japan and Indonesia. Over the U.S.A., the largest impact over the central Pacific was caused by including the Kilauea volcano and its impacts on the continental U.S.A. was limited to the western U.S.A. during the summer. The emissions from the Soufriere Hills volcano located in Montserrat affected the southern U.S.A. during the winter season. Analysis of temporal variations at measurement sites located in Hawaii and Florida showed improvements in modeling performance as a result of inclusion of volcanic SO_2 emissions. The changes in simulated aloft SO_4^{2-} concentration were investigated, and it was revealed that the impact were detected up to the top of the free troposphere although the considered SO_2 emissions were injected in the lower and middle of the free troposphere.

The results suggest that emissions of SO_2 resulting from volcanic degassing is one of the important sources that should be considered in the modeling system as it regulates tropospheric SO_4^{2-} levels not only in the vicinity of the volcano but also through long-range transport that modulates background levels at downwind continents. In addition to inclusion of

https://doi.org/10.5194/gmd-2021-109
Preprint. Discussion started: 4 May 2021

persistent degassing emissions, eruptive volcanic emissions can also play an important role in episodically modulating tropospheric sulfur budgets. As seen from the analysis of model and measured values at the Kilauea volcanic site in this study, the approach to treat the degassing volcanic SO_2 emissions as assigned in one model vertical layer without any temporal variation sometimes lead to the unexpected positive bias on cleaner days. A more realistic treatment of temporal variation of degassing gasses and the related meteorological parameters (e.g., local wind speed) would be useful to further refine the modeling performance of SO_4^{2-} produced via volcanic SO_2 emission.

Code availability

Source code for version 5.2 of the CMAQ model can be downloaded from https://github.com/USEPA/CMAQ/tree/5.2. For further information, please visit the U.S. Environmental Protection Agency website for the CMAQ system: https://www.epa.gov/cmaq.

Data availability

The observational datasets used in this study are available from their respective websites: http://www.eanet.asia/index.html (EANET), https://www.epa.gov/castnet (CASTNET), and http://vista.cira.colostate.edu/Improve (IMPROVE) for surface observation network. Last Access: 31 August 2020.
The emissions for original H-CMAQ simulation and degassing volcanic SO_2 emissions established in this study can be available upon the request.

Competing interests

The authors declare that they have no conflict of interest.

Disclaimer

The views expressed in this paper are those of the authors and do not necessarily reflects the views or policies of the U.S. Environmental Protection Agency.

https://doi.org/10.5194/gmd-2021-109
Preprint. Discussion started: 4 May 2021

Author contributions

Syuichi Itahashi performed the incorporation of degassing volcanic SO_2 emissions, analysis of observations and model simulation results, and prepared the manuscript with contributions from all co-authors. Rohit Mathur, Christian Hogrefe, and Sergey L. Napelenok contributed to establish the hemispheric modeling application for this study and prepared the original emission dataset and initial condition from previous long-term simulation results. Yang Zhang contributed to the literature review and refined this research through simulation designs, and result analyses and interpretation.

Acknowledgement

We thank Golam Sarwar and Barron Henderson for constructive suggestions on the initial version of this manuscript. The authors are grateful for the available observation dataset (EANET, IMPROVE, and CASTNET). Yang Zhang acknowledges support from the 2019-2020 North Carolina State University's Kelly Memorial Fund for US-Japan Scientific Cooperation.

References

Acid Deposition Monitoring Network in East Asia (EANET): http://www.eanet.asia/index.html, Last Access: 1 September 2020.

Andres, R.J. and Kasgnoc, A.D.: A time-averaged inventory of subaeroal volcanic sulfur emissions, J. Geophys. Res., 103, D19, 25251–25261, 2012.

Appel, K.W., Napelenok, S., Foley, K.M., Pye, H.O.T., Hogrefe, C., Luecken, D.J., Bash, J.O., Roselle, S.J., Pleim, J.E., Foroutan, H., Hutzell, W., Pouliot, G., Sarwar, G., Sarwar, G., Fahey, K., Gantt, B., Gilliam, R.C., Kang, D., Mathur, R., Schwede, D., Spero, T., Wong, D.C., & Young, J.: Overview and evaluation of the Community Multiscale Air Quality (CMAQ) model version 5.1. Geosci. Model Dev., 10, 1703–1732, doi:10.5194/gmd-10-1703-2017, 2017.

Carn, S.A., Clarisse, L., and Prata, A.J.: Multi-decadal satellite measurements of global volcanic degassing, J. of Volcanology and Geothermal Research, 311, 99-134, doi:10.1016/j.volgeores.2016.01.002, 2016.

Carn, S.A., Fioletov, V.E., McLinden, C.A., Li, C.and Krotkov, N.A.: A decade of global volcanic SO_2 emissions measured from space, Scientific Reports, 7, 44095, doi:10.1038/srep44095, 2017.

Chatani, S., Shimadera, H., Itahashi, S., and Yamaji, K.: Comprehensive analyses of source sensitivities and apportionments of $PM_{2.5}$ and ozone over Japan via multiple numerical techniques. Atmos. Chem. Phys., 20, 10311–29, 2020.

Chen, L., Gao, Y., Zhang, M., Fu, J.S., Zhu, J., Liao, H., Li, J., Huang, K., Ge, B., Wang, X., Lam, Y. F., Lin, C-Y., Itahashi, S., Nagashima, T., Kajino, M., Yamaji, K., Wang, Z., and Kurokawa, J.: MICS-Asia III: multi-model comparison and evaluation of aerosol over East Asia. Atmos. Chem. Phys., 19, 11911–11937, 2019.

https://doi.org/10.5194/gmd-2021-109
Preprint. Discussion started: 4 May 2021

Chin, M., Jacob, D.J., Gardner, G.M., Foreman-Fowler, M.S., Spiro, P.A. and Savoie D.L.: A global three-dimensional model of tropospheric sulfate, J. Geophys. Res.: Atmospheres, 101, 18667–18690, 1996.

Chin, M. and Jacob, D.J.: Anthropogenic and natural contributions to tropospheric sulfate: A global model analysis, J. Geophys. Res.: Atmospheres, 101, 18691–18699, 1996.

Clean Air Status and Trends Network (CASTNET), U.S. Environmental Protection Agency Clean Air Markets Division: https://www.epa.gov/castnet, Last Access: 1 September 2020.

Emery, C., Liu, Z., Russell, A. G., Odman, M. T., Yarwood, G., and Kumar, N.: Recommendations on statistics and benchmarks to assess photochemical model performance, J. of the Air and Waste Manage. Assoc., 67, 582–598, doi:10.1080/10962247.2016.1265027, 2017.

Galmarini, S., Koffi., B., Solazzo, E., Keating, T., Hogrefe, C., Schulz, M., Benedictow, A., Griesfeller, J. J., Janssens-Maenhout, G., Carmichael, G., Fu, J., and Dentener, F.: Technical note: Coordination and harmonization of the multi-scale multi-model activities HTAP2, AQMEII3, and MICS-Asia3: simulations, emission inventories, boundary conditions, and model output formats, Atmos. Chem. Phys., 17, 1543–1555, doi:10.5194/acp-17-1543-2017, 2017.

Gan, C.-M., Pleim, J., Mathur, R., Hogrefe, C., Long, C. N., Xing, J., Wong, D., Gilliam, R., and Wei, C.: Assessment of long-term WRF-CMAQ simulations for understanding direct aerosol effects on radiation "brightening" in the United States, Atmos. Chem. Phys., 15, 12193–12209, doi:10.5194/acp-15-12193-2015, 2015.

Ge, C., Wang, J., Carn, C., Yang, K., Ginoux, P. and Krotkov, N.: Satellite-based global volcanic SO_2 emissions and sulfate direct radiative forcing during 2005-2012, J. of Geophys. Res. Atmos., 121, 3446–3464, doi:10.1002/2015JD023134, 2015.

Hand, J.L., Schichtel., B.A., Malm, W.C., Pitchford, M. L.: Particulate sulfate ion concentration and SO2 emission trends in the United States from the early 1990s through 2010, Atmos. Chem. Phys., 12, 10353–10365, doi:10.5194/acp-12-10353-2012, 2012.

Hogrefe, C., Liu., P., Pouliot, G., Mathur, R., Roselle, S., Flemming, J., Lin, M., and Park, R. J.: Impacts of different characterizations of large-scale background on simulated regional-scale ozone over the continental United States, Atmos. Chem. Phys., 18, 3839–3864, doi:10.5194/acp-18-3839-2018, 2018.

Iacono, M. J., Delamere, J. S., Mlawer, E. J., Shephard, M. W., Clough, S. A., and Collins, W. D.: Radiative forcing by long-lived greenhouse gases: Calculations with the AER radiative transfer models, J. Geophys. Res., 113, D13103, doi:10.1029/2008JD009944, 2008.

Integrated Monitoring of Protected Visual Environments (IMPROVE), http://vista.cira.colostate.edu/Improve, Last Access: 1 September 2020.

Itahashi, S., Hayami, H., Yumimoto, K., and Uno, I.:. Chinese province-scale source apportionments for sulfate aerosol in 2005 evaluated by the tagged tracer method, Environ. Pollut., 220, 1366–1375, 2017a.

https://doi.org/10.5194/gmd-2021-109
Preprint. Discussion started: 4 May 2021

Itahashi, S., Hatakeyama, S., Shimada, K., Tatsuta, S., Taniguchi, Y., Chan, C.K., Kim, Y.P., Lin, N.-H. and Takami, A.: Model estimation of sulfate aerosol source collected at Cape Hedo during an intensive campaign in October-November, 2015, Aerosol and Air Quality Research, 17, 3079–3090, doi:10.4209/aaqr.2016.12.0592, 2017b.

Itahashi, S.: Toward synchronous evaluation of source apportionments for atmospheric concentration and deposition of sulfate aerosol over East Asia, J. Geophys. Res.: Atmospheres, 123, 2927–2953, doi:10.1002/2017JD028110, 2018.

Itahashi, S., Yamaji, K., Chatani, S., and Hayami, H.: Refinement of modeled aqueous-phase sulfate production via the Fe- and Mn-catalyzed oxidation pathway, Atmosphere, 9, 132, doi:10.3390/atmos9040132, 2018.

Itahashi, S., Hatakeyama, S., Shimada, K. and Takami, A.: Sources of high sulfate aerosol concentration observed at Cape Hedo in spring 2012, Aerosol and Air Quality Research, 19, 587–600, doi:10.4209/aaqr.2018.09.0350, 2019.

Itahashi, S., Mathur, R., Hogrefe, C. and Zhang, Y.: Modeling stratospheric intrusion and trans-Pacific transport on tropospheric ozone using hemispheric CMAQ during April 2010 – Part 1: Model evaluation and air mass characterization for stratosphere-troposphere transport, Atmos. Chem. Phys., 20, 3373–3396, doi:10.5194/acp-20-3373-2020, 2020a.

Itahashi, S., Mathur, R., Hogrefe, C., Napelenok, S.L. and Zhang, Y.: Modeling stratospheric intrusion and trans-Pacific transport on tropospheric ozone using hemispheric CMAQ during April 2010 – Part 2: Examination of emission impacts based on the higher-order decoupled direct method, Atmos. Chem. Phys., 20, 3397–3413, doi:10.5194/acp-20-3397-2020, 2020b.

Janjic, Z.: The step-mountain Eta coordinate Model: Further developments of the convection, viscous sublayer, and turbulence closure schemes , Month. Wet. Rev., 122, 927−945, 1994.

Janssens-Maenhout, G., Crippa, M., Guizzardi, F., Dentener, F., Muntean, M., Pouliot, G., Keating, T., Zhang, Q., Kurokawa, J., Wankmuller, R., Danier van der Gon, H., Kuenen, J.J.P., Kilmont, Z., Frost, G., Darras, S., Koffi, B. and Li, M.: HTAP_v2.2: a mosaic of regional and global emission grid maps for 2008 and 2010 to study hemispheric transport of air pollution. Atmos. Chem. Phys. 15: 11411–11432, doi:10.5194/acp-15-11411-2015, 2015.

Kain, J. S.: The Kain-Fritsch convective parameterization: An update, J. Appl. Meteor., 43, 170-181, 2004.

Kroll, J.H., Cross, E.S, Hunter, J.F., Pai, S., XII, T., XI, T., Wallace, L.M.M., Croteau, P.L., Jayne, J.T., Worsnop, D.R., Heald, C.L., Murphy, J.G. and Frankel, S.L.: Atmospheric evolution of sulfur emissions from Kilauea: Real-time measurements of oxidation, dilution, and neutralization within a volcanic plume, Environ. Sci. Tech., 49, 4129–4137, doi:10.1021/es506119x, 2015.

Lamotte, C., Guth, J., Marecal, V. B. and Cussac, M.: Modeling study of the impact of SO_2 volcanic passive emissions on the tropospheric sulfur budget. Atmos. Chem. Phys. Discuss. In review. Doi.10.5194/acp-2020-1040. 2020.

Li, M., Liu, H., Geng, G., Hong, C., Liu, F., Song, Y., Tong, D., Zheng, B., Cui, H., Man, H., Zhang, Q., and He, K.: Anthropogenic emission inventories in China: a review, Nat. Sci. Rev., 4, 834–866, 2017.

Liu, J., Mauzerall, D.L., and Horowitz, L.W.: Source-receptor relationships between East Asian sulfur dioxide emissions and Northern Hemisphere sulfate concentration, Atmos. Chem. Phys., 8, 3321–3733, 2008.

https://doi.org/10.5194/gmd-2021-109
Preprint. Discussion started: 4 May 2021

Mathur, R., Xing, J., Gilliam, R., Sarwar, G., Hogrefe, C., Pleim, J., Poliot, G., Roselle, S., Spero, T. L., Wong, D. C., and Young, J.: Extending the Community Multiscale Air Quality (CMAQ) modeling system to hemispheric scales: overview of process considerations and initial applications, Atmos. Chem. Phys., 17, 12449–12474, doi:10.5194/acp-17-12449-2017, 2017.

Mathur, R., Zhang, Y., Hogrefe, C., and Xing, J.: Long-terms trends in sulfur and reactive nitrogen deposition across the Northern Hemisphere and United States, in Mensink, C, Gong, W., Hakami, A. (eds.), Air Pollution Modeling and Its Application XXVI, ITM 2018, Springer Proceedings in Complexity, Springer, Cham., https://doi.org/10.1007/978-3-030-22055-6_7, 2020.

McCormick, M.P., Thomason, L.W., and Trepte, C.R.: Atmospheric effects of the Mt Pinatubo eruption, Nature, 373, 2, 1995.

Morrison, H., Thompson, G., Tatarskii, V.: Impacts of cloud microphysics on the development of trailing stratiform precipitation in a simulated squall line: comparison of one- and two-moment schemes. Monthly Weather Rev. 137, 991-1007, 2009

National Centers for Environmental Prediction (NCEP): Final (FNL) Operational Global Analysis data, available at: available at: https://rda.ucar.edu/datasets/ds083.2/, last access: 1 October 2020.

Pouliot, G., Denier van der Gon, H. A. C., Kuenen, J., Zhang, J., Moran, M. D., and Maker, P. A.: Analysis of the emission inventories and model-ready emission datasets of Europe and North America for phase 2 of the AQMEII project, Atmos. Environ., 115, 345-360, doi:10.1016/j.atmosenv.2014.10.061, 2015.

Sarwar, G., Gantt, B., Schwede, D., Foley, K., Mathur, R., and Saiz-Lopez, A.: Impact of enhanced ozone deposition and halogen chemistry on tropospheric ozone over the Northern Hemisphere, Environ. Sci. Tech., 49, 9203–9211, doi:10.1021/acs.est.5b01657, 2015.

Seinfeld, J. H. and Pandis, S. N.: *Atmospheric Chemistry and Physics—From Air Pollution to Climate Change*, 3rd ed.; John Wiley & Sons: New York, 2016.

Simon, H. and Bhave, P.V.: Simulating the degree of oxidation in atmospheric organic particles, *Environ. Sci. Technol., 46*(1): 331-339. doi: 10.1021/es202361w, 2012.

Smith, S.J., van Aardenne, J., Klimont, Z., Andres, R.J., Volke, A., Arias, S.D.: Anthropogenic sulfur dioxide emissions: 1850-2005, Atmos. Chem. Phys., 11, 1101–1116, doi:10.5194/acp-11-1101-2011, 2011.

Smithsonian Institution, National Museum of Natural History, Global Volcanism Program, https://volcano.si.edu, Last Acess: 31 August, 2020

Tang, Y., Tong, D.Q., Yang, K., Lee, P., Baker, B., Crarwford, A., Luke, W., Stein, A., Campbell, P.C., Ring, A., Flynn, J., Wang, Y., McQueen, J., Pan, L., Huang, J. and Stajner, I.: Air quality impacts of the 2018 Mt. Kilauea volcano eruption in Hawaii: A regional chemical transport model study with satellite-constrained emissions, Atmos. Environ., 227, 117648, doi:10.1016/j.atmosenv.2020.117648, 2020.

Warneck, P. and Williams, J.: *The Atmospheric Chemist's Companion*; Springer: New York, 2012.

Western Regional Air Partnership (WRAP), https://www.wrapair2.org/default.aspx, Last Access: 1 September 2020.

https://doi.org/10.5194/gmd-2021-109
Preprint. Discussion started: 4 May 2021

Wild, M.: Global dimming and brightening: A review, J. Geophys. Res.-Atmos., 114, D00D16, https://doi.org/10.1029/2008JD011470, 2009.

Xing, J., Mathur, R., Pleim, J., Hogrefe, C., Gan, C.-M., Wong, D. C., Wei, C., Gilliam, R., and Pouliot, G.: Observations and modeling of air quality trends over 1990-2010 across the Northern Hemisphere: China, the United States and Europe, Atmos. Chem. Phys., 15, 2723–2747, doi:10.5194/acp-15-2723-2015, 2015a.

Xing, J., Mathur, R., Pleim, J., Hogrefe, C., Gan, C.-M., Wong, D. C., Wei, C. and Wang, J.: Air pollution and climate response to aerosol direct radiative effects: A modeling study of decadal trends across the northern hemisphere, J. Geophys. Res. Atmos., 120, 12,221–12,236, doi:10.1002/2015JD023933, 2015b.

Xing, J., Wang, J., Mathur, R., Pleim, J., Wang, S., Hogrefe, C., Gan, C.M., Wong, D.C. and Hao, J.: Unexpected benefits of reducing aerosol cooling effects. Environmental Science & Technology, 50(14), pp.7527-7534, 2016.

Yamaji, K., Chatani, S., Yamaji, K., Itahashi, S., Saito, M., Takigawa, M., Morikawa, T., Kanda, I., Miya, Y., Komatsu, H., Sakurai, T., Morino, Y., Nagashima, T., Kitayama, K., Shimadera, H., Uranichi, K., Fujiwara, Y., Shintani, S., and Hayami, H.: Model inter-comparison for $PM_{2.5}$ components over urban areas in Japan in the J-STREAM framework. Atmosphere, 11, 223, 2020.

Zhang, Q., Jimenez, J.L., Canagaratna, M.R., Allan, J.D., Coe, H., Ulbrich, I., Alfarra, M.R., Takami, A., Middlebrook, A.M., Sun, Y.L., Dzepina, K., Dunlea, E., Docherty, K., DeCarlo, P.F., Salcedo, D., Onasch, T., Jayne, J.T., Miyoshi, T., Shimono, A., Hatakeyama, S., Takegawa, N., Kondo, Y., Schneider, J., Drewnick, F., Borrmann, S., Weimer, S., Demerjian, K., Williams, P., Bower, K., Bahreini, R., Cottrell, L., Griffin, R.J., Rautiainen, J., Sun, J.Y., Zhang, Y.M., Worsnop, D.R.: Ubiquity and dominance of oxygenated species in organic aerosols in anthropogenically-influenced Northern Hemisphere midlatitudes. Geophys. Res. Lett., 34, L13801, 2007.

Zhang, Y., Liu, P., Pun, B., and Seigneur, C.: A Comprehensive Performance Evaluation of MM5-CMAQ for the Summer 1999 Southern Oxidants Study Episode, Part-I. Evaluation Protocols, Databases and Meteorological Predictions, Atmos. Environ., 40, 4825-4838, doi:10.1016/j.atmosenv.2005.12.043, 2006.

Zhang, Y., K. Vijayaraghavan, X.-Y. Wen, Snell, H. E. and Jacobson, M. Z.: Probing into regional ozone and particulate matter pollution in the United States: 1. A 1 year CMAQ simulation and evaluation using surface and satellite data, J. Geophys. Res., 114, D22304, doi:10.1029/2009JD011898, 2009.

Zhang, Y., Olsen, K.M., and Wang, K.: Fine scale modelling of agricultural air quality over the southeastern United States using two air quality models. Part I. Application and evaluation, Aerosol and Air Quality Research, 13, 1231-1252, doi:10.4209/aaqr.2012.12.0346, 2013.

Zhang, Y., Mathur, R., Bash, J. O., Hogrefe, C., Xing, J., and Roselle, S.J.: Long-term trends in total inorganic nitrogen and sulfur deposition in the US from 1990 to 2010, Atmos. Chem. Phys., 18, 9091–9106, https://doi.org/10.5194/acp-18-9091-2018, 2018.

https://doi.org/10.5194/gmd-2021-109
Preprint. Discussion started: 4 May 2021

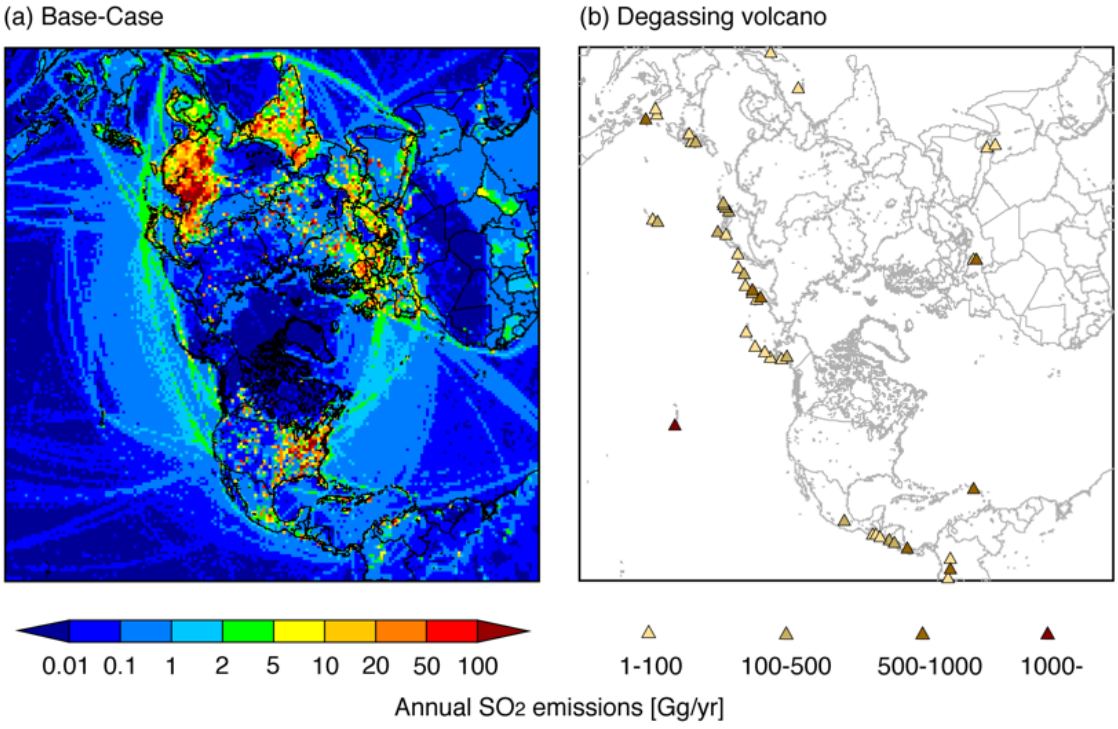

Figure 1. Geographical mapping of the (a) original SO_2 emissions used in H-CMAQ and (b) degassing volcanic annual SO_2 emissions incorporated in this study during 2010.

https://doi.org/10.5194/gmd-2021-109
Preprint. Discussion started: 4 May 2021

Geoscientific Model Development
Discussions
Open Access
EGU

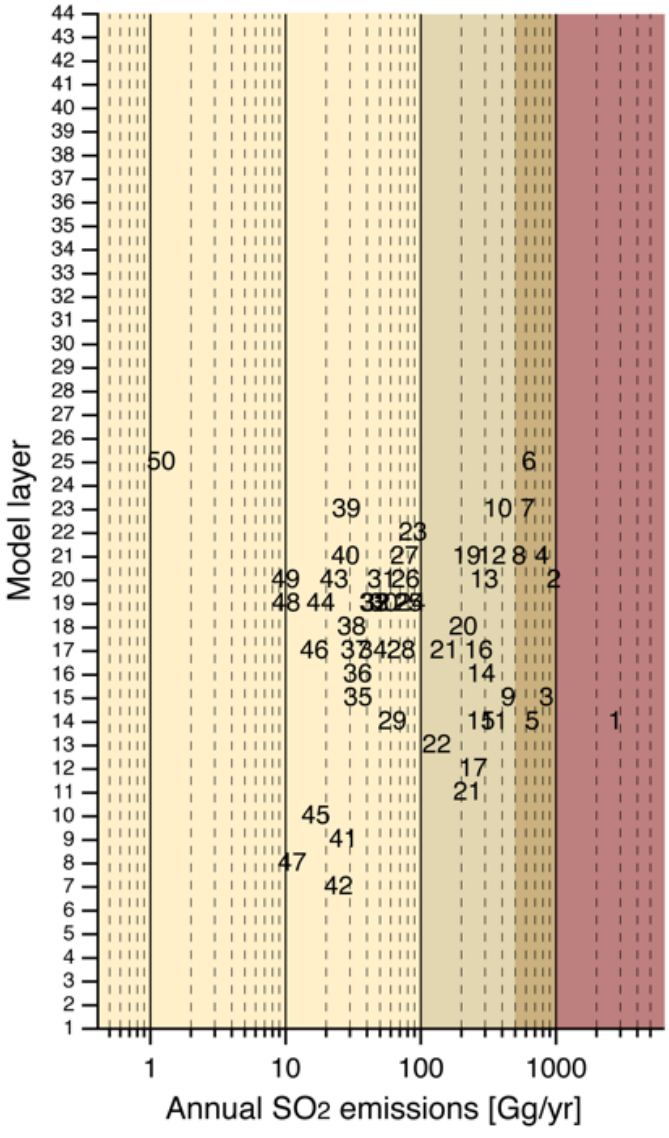

Figure 2. The model layers to which the SO_2 emissions from the 50 volcanoes considered in this study were assigned. See Table 1 for a listing of the volcanoes represented by each number in this Figure. In Table 1, volcanoes are listed in decreasing order of their annual SO_2 emission amount.

https://doi.org/10.5194/gmd-2021-109
Preprint. Discussion started: 4 May 2021

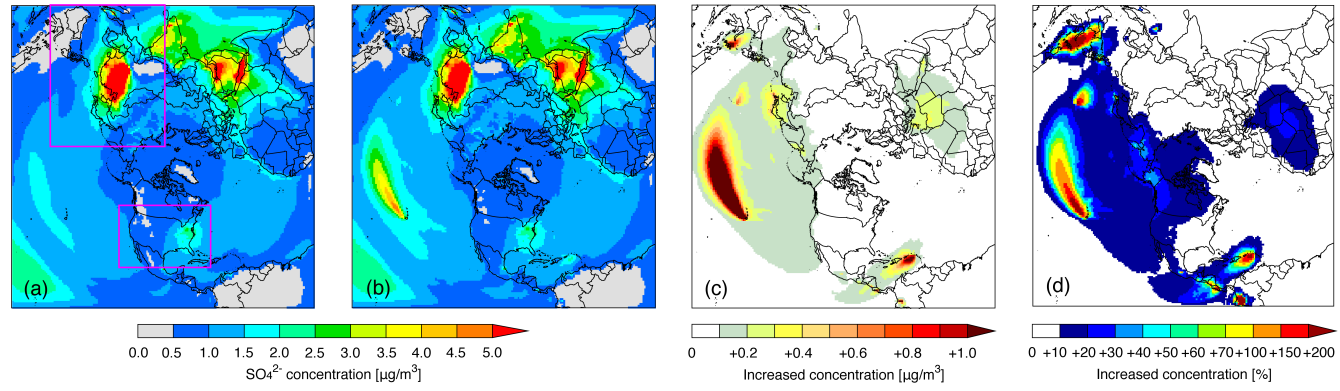

Figure 3. Simulated annual averaged SO_4^{2-} concentration in 2010 by (a) original H-CMAQ and (b) H-CMAQ with incorporation of volcanic SO_2 emissions, (c) increased concentration by the incorporation of volcanic SO_2 emissions, and (d) same as (c) but shown as relative percentages at the surface. The rectangular regions colored in pink in panel (a) indicate the Asia (left-top) and U.S.A. (right-bottom) subdomains used for detailed analysis.

https://doi.org/10.5194/gmd-2021-109
Preprint. Discussion started: 4 May 2021

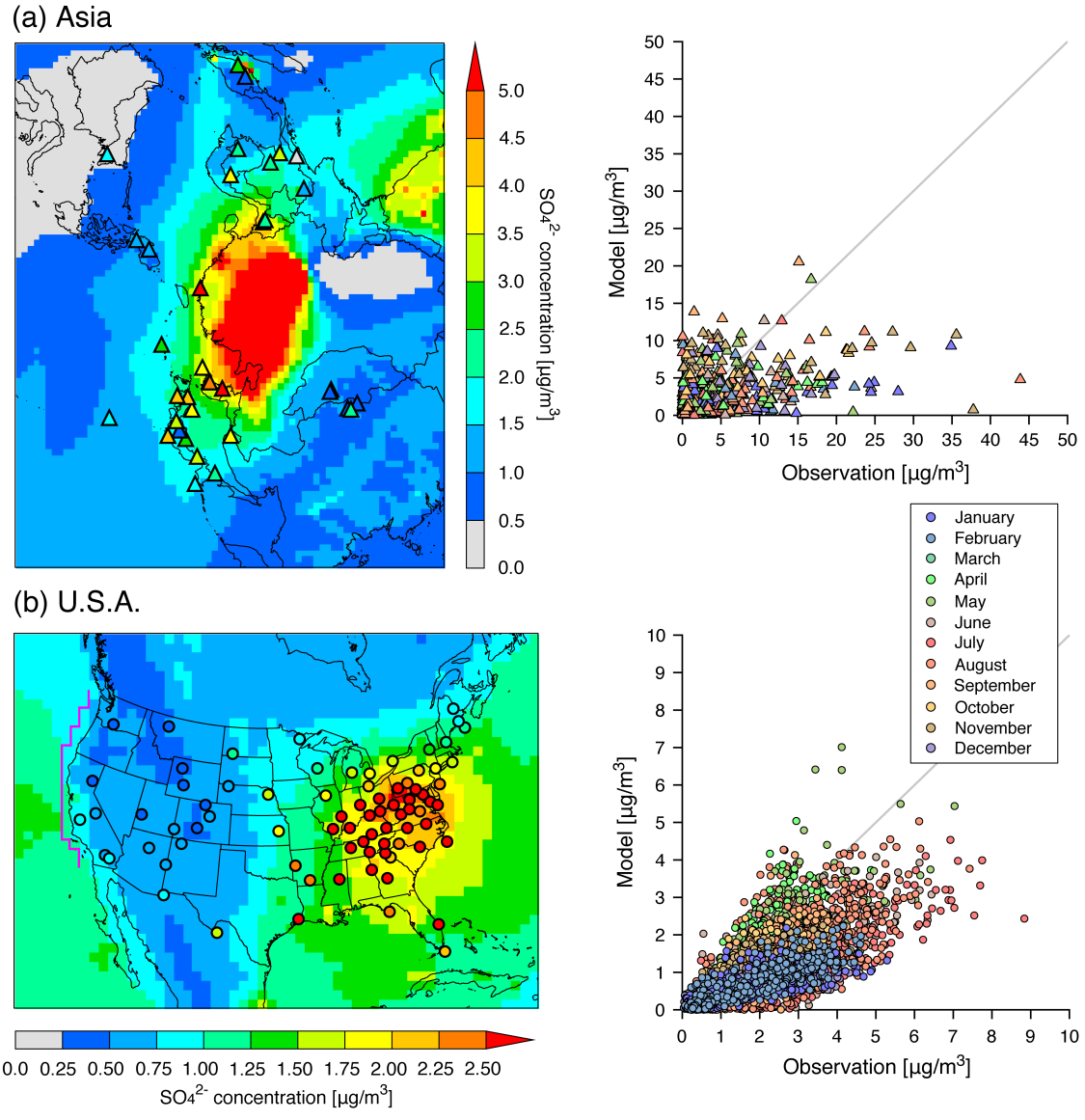

Figure 4. Simulated annual averaged SO_4^{2-} concentration in 2010 by original H-CMAQ over (a) Asia and (b) U.S.A. with overlaid EANET and CASTNET surface observations. Scatter-plots between surface observation (EANET over Asia, and CASTNET over U.S.A.) and original H-CMAQ with identification colors for each month is also shown. Note that the color-scale is different for Asia and U.S.A. The pink line over the western U.S.A. in panel (b) is the defined western edge to analyze the vertical profile of SO_4^{2-} concentrations (see, Fig. 7).

https://doi.org/10.5194/gmd-2021-109
Preprint. Discussion started: 4 May 2021

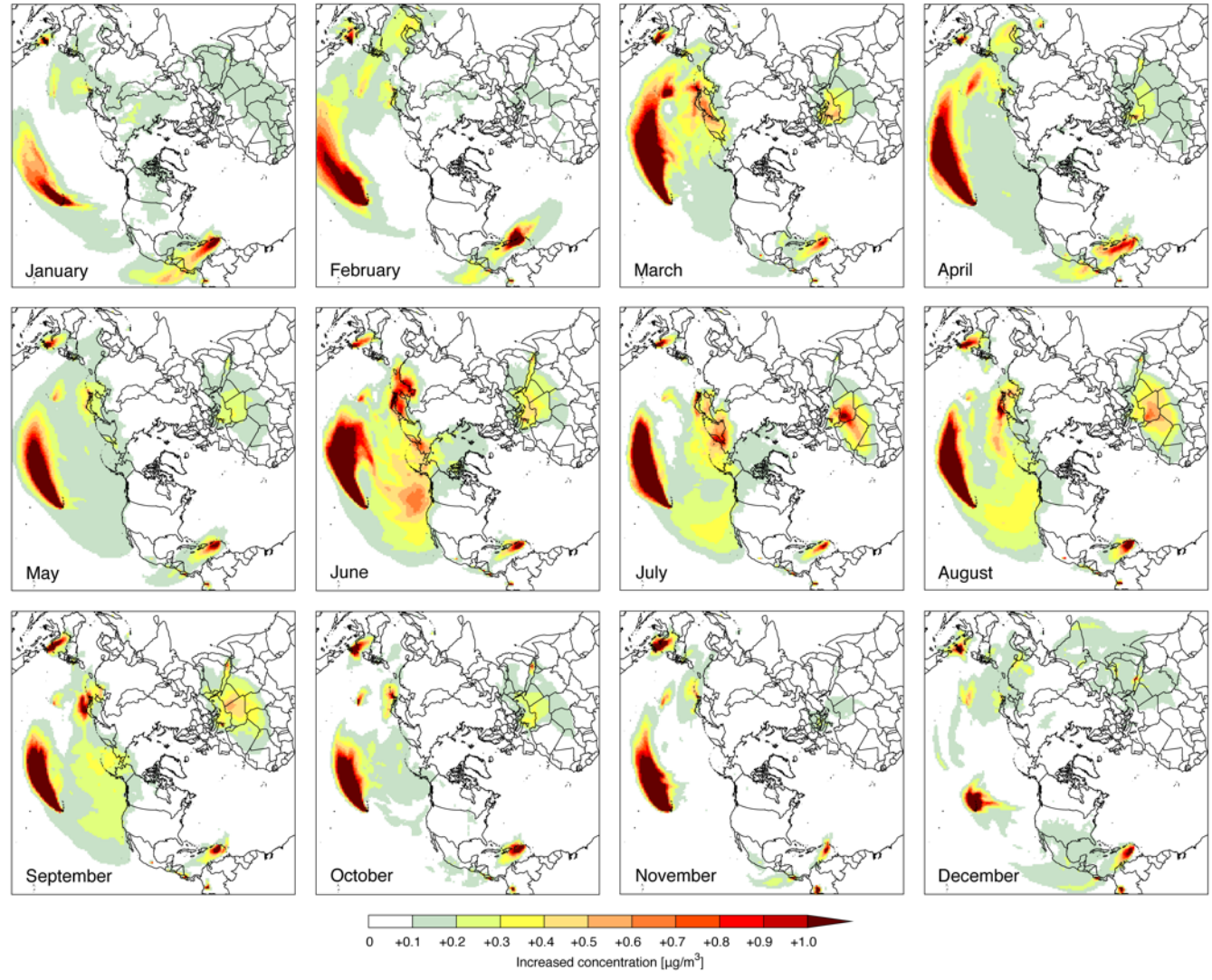

Figure 5. Simulated increased surface SO_4^{2-} concentration by the incorporation of volcanic SO_2 emissions over each month in 2010 at surface.

https://doi.org/10.5194/gmd-2021-109
Preprint. Discussion started: 4 May 2021

Geoscientific Model Development Discussions

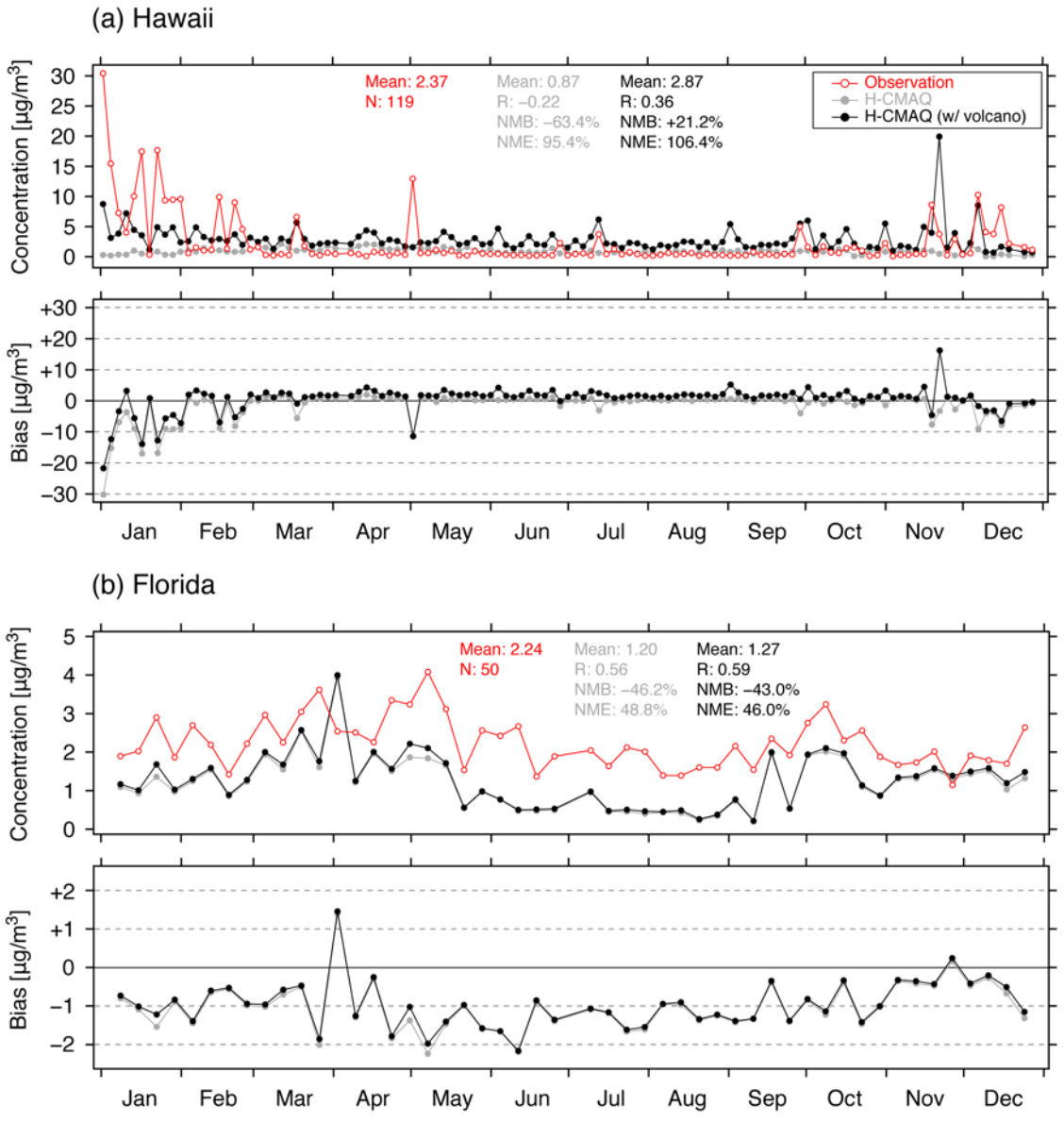

Figure 6. Temporal variation of observed and simulated SO_4^{2-} concentrations and simulation biases at (a) Hawaii IMPROVE site (HAVO1) and (b) Florida CASTNET site (EVE419) in 2010. Red open circle denotes observations, and gray and black closed circles denote original H-CMAQ and H-CMAQ incorporating volcanoes, respectively. Statistical scores are indicated in the inset.

https://doi.org/10.5194/gmd-2021-109
Preprint. Discussion started: 4 May 2021

Geoscientific Model Development Discussions
Open Access
EGU

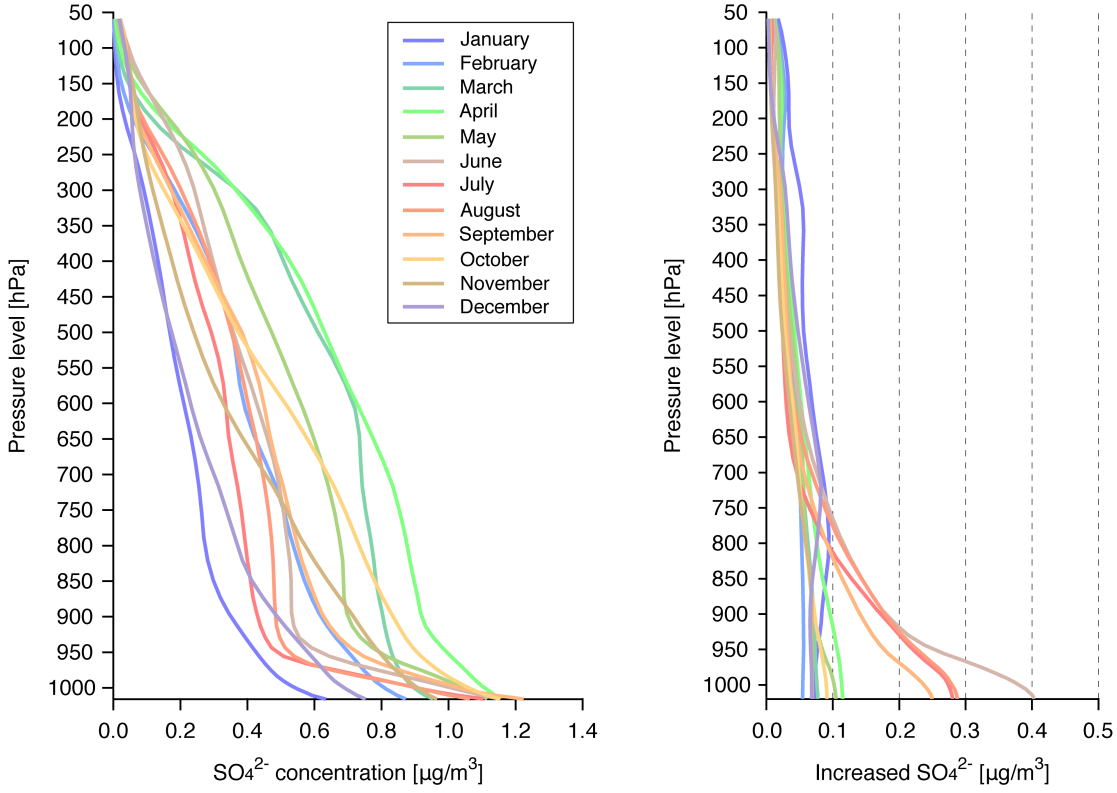

Figure 7. Vertical profile of simulated SO_4^{2-} concentration of each month in 2010 at the edge of western U.S.A. (see, Fig. 4) (left) original H-CMAQ and (right) increased concentration by the incorporation of volcanic SO_2 emissions.

5

https://doi.org/10.5194/gmd-2021-109
Preprint. Discussion started: 4 May 2021

Geoscientific Model Development Discussions
Open Access
EGU

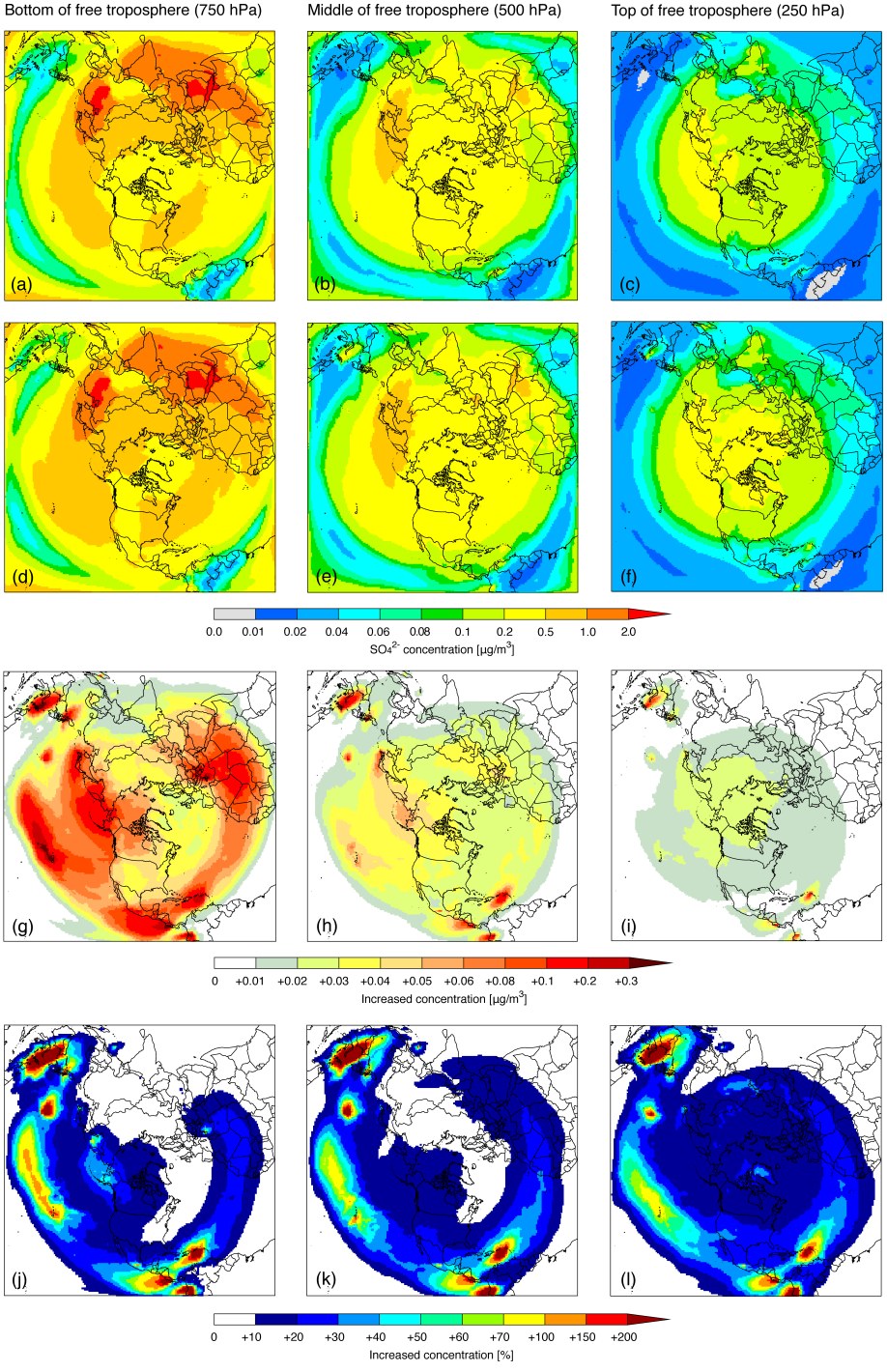

Figure 8. Simulated annual averaged SO_4^{2-} concentration in 2010 by (a-c) original H-CMAQ and (d-f) H-CMAQ with incorporation of volcanic SO_2 emissions, (g-i) increased concentration by the incorporation of volcanic SO_2 emissions, and (j-l) same as (g-i) but shown as relative percentage at the bottom of the free troposphere (750 hPa; a, d, g, j), middle of the free troposphere (500 hPa; b, e, h, k), and top of the free troposphere (250 hPa; c, f, I, l).

https://doi.org/10.5194/gmd-2021-109
Preprint. Discussion started: 4 May 2021

Geoscientific Model Development Discussions

Table 1. Information of volcanoes incorporated in this study.

No.	Name	Country	Longitude [°]	Latitude [°]	Altitude [m a.s.l]	Emission [Gg/yr]
1	Kilauea	USA	-155.29	19.42	1222.0	2739.0
2	Mutnovsky + Gorely	Russia	158.20	52.45	2322.0	960.4
3	Dukono	Indonesia	127.88	1.68	1170.0	848.9
4	Turrialba + Poas	Costa Rica	-83.77	10.03	3340.0	788.5
5	Soufriere Hills	Montserrat (UK)	-62.18	16.72	870.0	667.1
6	Kliuchevskoi + Bezymianny	Russia	160.64	56.06	4835.0	631.2
7	Nevado del Huila	Colombia	-76.03	2.93	5364.0	617.6
8	Etna	Italy	15.00	37.73	2711.0	533.3
9	Sakura-jima	Japan	130.65	31.59	1117.0	443.5
10	Popocatepetl	Mexico	-98.62	19.02	5100.0	372.1
11	Suwanose-jima	Japan	129.71	29.64	796.0	349.3
12	Shiveluch	Russia	161.34	56.64	3283.0	334.7
13	Mayon	Philippines	123.69	13.26	2462.0	293.7
14	Karymsky	Russia	159.45	54.05	1536.0	280.2
15	Miyake-jima	Japan	139.53	34.09	775.0	276.7
16	Sarychev	Russia	153.21	48.08	1200.0	267.3
17	Pagan	Northern Mariana Islands	145.79	18.14	570.0	244.5
18	Masaya	Nicaragua	-86.16	11.98	635.0	221.3
19	Avachinsky	Russia	158.83	53.25	2741.0	218.1
20	San Cristobal +Telica	Nicaragua	-87.00	12.70	1745.0	206.0
21	Aso	Japan	131.10	32.88	1592.0	149.2
22	Satsuma-Iojima	Japan	130.31	30.79	704.0	131.0
23	Shishaldin	USA	-163.97	54.76	2857.0	87.4
24	Chikurachki + Ebeko	Russia	155.46	50.33	1816.0	85.0
25	Asama	Japan	138.52	36.41	2568.0	80.3
26	Fuego + Pacaya	Guatemala	-90.88	14.47	3763.0	77.0
27	Redoubt	USA	-152.75	60.49	3108.0	75.7
28	Bulusan	Philippines	124.05	12.77	1500.0	71.5
29	Stromboli	Italy	15.21	38.79	870.0	61.6
30	Karangetang	Indonesia	125.40	2.78	1780.0	53.3
31	Santa Maria	Guatemala	-91.55	14.76	3772.0	51.5
32	Sinabung	Indonesia	98.39	3.17	2460.0	46.4
33	Tokachi	Japan	142.69	43.42	2077.0	45.0
34	Lokon-Empung	Indonesia	124.79	1.36	1580.0	44.4
35	Ketoi	Russia	152.48	47.34	870.0	34.3
36	Kudriavy	Russia	148.84	45.39	1125.0	34.1
37	Augustine	USA	-153.45	59.35	1252.0	32.8
38	Gareloi	USA	-178.79	51.79	1573.0	30.9
39	Spurr	USA	-152.25	61.30	3374.0	28.2
40	Veniaminof	USA	-159.38	56.17	2507.0	27.7
41	Anatahan	Northern Mariana Islands	145.67	16.35	320.0	26.8
42	Barren Island	India	93.86	12.28	230.0	24.6
43	Galeras	Colombia	-77.39	1.20	4276.0	22.8
44	Santa Ana	El Salvador	-89.63	13.85	2381.0	18.2
45	Alu-Dalafilla + Erta Ale	Ethiopia	40.67	13.60	613.0	16.7
46	Cleveland	USA	-169.77	52.83	1170.0	16.3

https://doi.org/10.5194/gmd-2021-109
Preprint. Discussion started: 4 May 2021


Geoscientific Model Development Discussions

47	Jebel-at-Tair	Yemen	41.83	15.55	244.0	11.2
48	Kizimen	Russia	160.36	55.12	2376.0	10.1
49	Kanlaon	Philippines	123.13	10.41	2435.0	10.0
50	Nevado del Ruiz	Colombia	-75.32	4.90	5321.0	1.2

https://doi.org/10.5194/gmd-2021-109
Preprint. Discussion started: 4 May 2021

Geoscientific Model Development Discussions

Table 2. Statistical analysis of modeled SO_4^{2-} concentration with observations.

	N	Mean		R	NMB	NME
		Observation	Model			
EANET						
−original H-CMAQ	1167	3.68	2.30	0.43^{***}	−37.6%	67.0%
−incorporation of volcanic emissions			2.44	0.43^{***}	−33.6%	66.0%
CASTNET						
−original H-CMAQ	4216	1.91	1.36	0.73^{***}	−28.7%	39.4%
−incorporation of volcanic emissions			1.42	0.73^{***}	−25.6%	38.6%
IMPROVE						
−original H-CMAQ	18844	1.05	0.94	0.64^{***}	−10.6%	53.9%
−incorporation of volcanic emissions			1.02	0.64^{***}	−3.2%	46.0%

Note: The unit of mean for observations and simulations is μg/m^3. Suggested threshold values of $R > 0.70$, $NMB < \pm 10\%$, and $NME < 35\%$ as performance goal, and threshold values of $R > 0.40$, $\pm 10\% < NMB < \pm 30\%$, and $35\% < NME < 50\%$ as performance criteria for daily SO_4^{2-} by the regional-scale modeling reviewed by Emery et al. (2017). Significance levels by Students' t-test for correlation coefficients between observations and simulations are remarked as $^{*}p < 0.05$, $^{**}p < 0.01$, and $^{***}p < 0.001$, and lack of a mark indicates no significance.